Nucleation Mechanism of α-Cyclodextrin-Enhanced Crystallization of Some Semicrystalline Aliphatic Polymers

Tungalag Dong, Yong He, Bo Zhu, Kyung-Moo Shin, and Yoshio Inoue*

Department of Biomolecular Engineering, Tokyo Institute of Technology, Nagatsuta 4259-B-55, Midori-ku, Yokohama 226-8501, Japan

Received April 19, 2005; Revised Manuscript Received July 11, 2005

ABSTRACT: The nucleation effects of α-cyclodextrin (α-CD) and its inclusion complexes (ICs) with poly(ϵ-caprolactone) (PCL), poly(ethylene glycol) (PEG), and poly(butylene succinate) (PBS) on the crystallization of PCL, PEG, and PBS were investigated by differential scanning calorimetry (DSC) and polarized optical microscopy. The formations of ICs of α-CD with PCL, PEG, and PBS were characterized by DSC, Fourier transform infrared spectroscopy, wide-angle X-ray diffraction (WAXD), and solution ^{1}H NMR. The WAXD studies showed that all of the α-CD-ICs adopt a channel structure. Both DSC and ^{1}H NMR results suggested that the polymer chains were partially complexed by α-CDs. Thus, the polymer chains in the bulk phase can contact not only the exterior of the α-CD macrocycle but also the end parts of polymer chains protruding from the α-CD cavity and/or the free chain segments uncovered by α-CD, when the α-CD-IC as a nucleating agent is added into the polymers. Therefore, the difference in the interfacial interaction between bulk polymers and the nucleating agents should be responsible for the difference in the nucleation effects. α-CD-PCL-IC particles have little nuclear formation effect on the crystallization of bulk PBS; however, they can greatly accelerate the nucleation and crystallization of the bulk PCL. The same results are also observed during the crystallization of PBS and PEG; that is, PBS-IC and PEG-IC particles can greatly accelerate the nucleation and crystallization of PBS and PEG, respectively. It seemed that IC of a given polymer could greatly enhance the nucleation and crystallization of the polymer itself. This result may be attributable to the limited mobility of the uncovered part of the polymer segments constrained by its interior part resided in the α-CD cavity, leading to the nucleation of polymer crystallization. The effect of fine talc powder was also examined. The experimental results suggested that the nucleation ability of α-CD on the crystallization of the polymer is comparable to that of the talc.

Introduction

The rapid development of polymer science and engineering and the wide applications of polymeric materials are obviously one of the characters of the last century. Especially, during the past several 10 years, the polymeric materials have contributed to the society very much. However, the wide applications of plastics also result in an irreversible buildup of polymer waste in the environment. Fortunately, biodegradable polymeric materials offer an attractive solution to alleviate the environmental concerns about the consequences of polymer waste accumulation. The biodegradable polymers could be easily biodegraded into simpler compounds, and after utilization by microorganisms, they are redistributed by elemental cycle such as the carbon and nitrogen cycles.[1] Hence, minimum environmental pollution is expected when such materials are disposed of after their use.

Among biodegradable polymers, the aliphatic polyesters are the most important category, which own similar mechanical and thermal properties to those traditional engineering plastics.[2] However, their application still suffers from some disadvantages, which varies with the polyester referred. Recently, much attention has been paid toward the improvement of properties of biodegradable polymers. Since Harada et al. found that a lot of α-cyclodextrins (α-CD) are threaded on a poly(ethylene glycol) (PEG) chain to form a crystalline inclusion complex (IC),[3] the formation and properties of ICs of CDs with various polymers have been studied to improve miscibility,[4] biodegradation,[5] and crystallization[6] of polymers. A representative of natural biodegradable polyesters is bacterial poly(3-hydroxybutyrate) (PHB) accumulated as intracellular energy reserves by a variety of microorganisms.[1,7] Bacterial PHB is produced by a fermentation process to produce extremely pure material after solvent extraction from bacterial cells, resulting in an unusually low nucleation density. Thus, the melt of highly pure PHB may undergo homogeneous nucleation, and the crystallization rate of PHB is so slow that the processability window of PHB is very narrow.[8,9] Furthermore, the low nucleation density results in the big size of PHB spherulites, which, in combination with the secondary crystallization, makes crystalline PHB materials brittle.[8,9] As is well-known, an addition of an appropriate nucleation agent can help to increase the nucleation density and promote the crystallization of polymers, and thus it is expected to inhibit the embrittlement and improve the processing efficiency of polymeric materials. Some inorganic compounds such as talc have been intensely used as nucleating agents for polymers.[10] Although talc is a very effective nucleation agent for most polymers, it is closely related to the potent carcinogen asbestos, which can induce tumors in the ovaries and lungs of cancer victims.[11]

From the viewpoint of environmental protection, green nucleating agents are desirable, especially for the biodegradable polymers. CDs are natural products, produced from a renewable natural material, starch, and are environmentally friendly.[12] In our previous

* To whom corresponding should be addressed. Tel: +81-45-924-5794. Fax: +81-45-924-5827. E-mail: yinoue@bio.titech.ac.jp.

10.1021/ma050826r CCC: $30.25
Published on Web 08/13/2005

works, it has been found that α-CD, as an effective nucleating agent, promotes the crystallization of PHB greatly.[9] It is reasonable to expect that α-CD can be used as a good nucleating agent for other biodegradable polymers. Further, we also wonder whether α-CD in ICs with polymers will benefit the nucleation of polymers or not. Furthermore, it is also speculated that α-CD can be used as a good nucleating agent for poly(butylene succinate) (PBS). PBS is a typical two-component aliphatic polyester composed of butane-1,4-diol and succinic acid and is considered to be one of the most accessible chemosynthesized aliphatic biodegradable polyesters.[13] However, the low nucleation density and the slow crystallization rate of PBS cause its relatively poor processability.[13]

In the present work, we will choose three kinds of semicrystalline polymers, poly(ϵ-caprolactone) (PCL), PEG, and PBS, as guest molecules in the α-CD-ICs, and these α-CD-ICs will be used as nucleating agents for the crystallization of the semicrystalline polymers. Also their nucleation effectiveness will be compared to the conventional nucleation agent, talc. The nucleation and crystallization behavior of PCL, PEG, and PBS with the nucleating agents will be investigated by a differential scanning calorimetry (DSC) and a polarized optical microscopy (POM). The possible nucleation mechanism of α-CD-enhanced crystallization behavior of semicrystalline polymers will be discussed.

Experimental Section

Materials. PEG with a number-average molecular weight M_n of 2.0×10^4 was purchased from Nacalai Tesque Inc., Japan. PBS ($M_n = 2.2 \times 10^4$, $M_w/M_n = 1.8$) and PCL ($M_n = 1.2 \times 10^4$, $M_w/M_n = 1.8$) were purchased form Showa Highpolymer Co., Ltd and Daicel Chemical Co., Japan, respectively. Before use, PEG and PBS (or PCL) were purified by precipitation, respectively, into *n*-heptane and ethanol from chloroform solutions. α-CD was supplied by Nihon Shokuhin Kako Co., Ltd., Japan. The talc powder was purchased form Kanto Kagaku Co., Ltd., Japan. The solvents, such as dimethyl sulfoxide (DMSO), acetone, and chloroform were purchased from Nacalai Tesque, Inc, Kyoto, Japan. The α-CD, talc and the solvents were used as received.

Sample Preparation. 1. α-CD-PCL-IC (PCL-IC).[14,15] PCL (0.4 g) and α-CD (4.0 g) were dissolved in acetone (150 mL) and distilled water (50 mL), respectively. The PCL solution was added slowly into the α-CD aqueous solution under vigorous stirring at 60 °C for 3 h. Subsequently, the solution was cooled to 25 °C and continuously stirred for further 24 h. The as-produced white powder was collected by filtration and then washed with acetone and water to remove free PCL and uncomplexed α-CD, respectively. Then, the final product was dried under vacuum at 60 °C for 1 week.

2. α-CD-PEG-IC (PEG-IC).[3] PEG (0.2 g) was mixed with a saturated aqueous solution (10 mL) of α-CD (1.0 g) at 25 °C, and the resulting solution was ultrasonically agitated (BRANSON−B3200 water bath, 47 kHz, 120W) at 25 °C for 15 min, followed by standing overnight at 25 °C. The precipitated product was washed with water and was dried under vacuum at 60 °C for 1 week.

3. α-CD-PBS-IC (PBS-IC).[16] α-CD (4.0 g) and PBS (0.25 g) were dissolved in DMSO (40 mL), and then the solution was stirred at 60 °C for 1 day. After adding an excess amount of chloroform (100 mL) into the mixture, the solution immediately became turbid. The precipitated products were filtrated and then washed by chloroform to remove free PBS. The remaining powder was dried under vacuum at 60 °C for 1 day, then washed with water to remove free α-CD, and again dried under vacuum at 60 °C for further 1 week.

4. Preparation of Polymer Samples Including Nucleating Agents. Considering the effect of the particle size of the nucleating agents on their abilities to nucleate crystallization of polymers (PCL, PEG, and PBS), the diminished size of the nucleating agents were prepared through shattering by ultrasonic treatment (BRANSON−B3200 water bath, 47 kHz, 120W) in the suspension with chloroform (for 10 min at 25 °C). The mixtures of polymer and nucleating agents were prepared by admixing 2 wt % of nucleating agents into a concentrated chloroform solution of polymer (0.1 g/mL); the solvent was then allowed to evaporate during rigorous stirring. The resultant films were dried at 25 °C under vacuum for 1 week before analysis. In Table 1 are shown the particle sizes of all nucleating agents measured by POM under molten state of polymer.

Table 1. Particle Size of Nucleation Agents

nucleation agent	particle size (μm)	ultrasonic treatment (min)	monomeric unit of polymer/ α-CD molar ratio (uncovered part of polymer)
α-CD	<5	10	
PCL-IC	<5	10	1.9:1 (47%)
PEG-IC	<5	10	5.7:1 (65%)
PBS-IC	<5	10	2.0:1 (70%)

Measurements. 1. Characterization of Inclusion Complexes. The Fourier transform infrared (FT-IR) spectrum was observed at 30 °C on a Perkin-Elmer Spectra 2000 single-beam IR spectrometer with a resolution of 4 cm^{-1}. The polymer samples for FT-IR measurement was prepared by casting 1.5 wt % chloroform solution on the surface of a silicon wafer. The solvent was completely evaporated under vacuum. The samples of α-CD and α-CD-ICs were pressed into KBr pellets, and the spectra were recorded with an accumulation of 16 scans at 30 °C.

The differential scanning calorimetry (DSC) thermograms of the sample (about 8 mg) pre-sealed into an aluminum pan was recorded on a Perkin-Elmer Pyris Diamond DSC. An indium standard was used for the calibration and nitrogen was used as the purge gas. The sample was heated to above melting temperature of polymers (90 °C for PCL and PEG, 140 °C for PBS), annealed for 5min, and then cooled to 0 °C at 10 °C min^{-1} (cooling scan), kept for 0 °C for 3min, finally then reheated to above melting temperature at 10 °C min^{-1} (heating scan).

The wide-angle X-ray diffraction (WAXD) pattern of the sample was recorded on a Rigaku RU-200 using Nickel-filtered Cu Kα radiation (40KV, 200mA) with the 2θ ranging from 5° to 35° at a scanning rate of one degree·min^{-1}.

Solution ^{1}H NMR spectra were recorded on a JEOL GSX270 NMR spectrometer in DMSO-d_6 at 80 °C. Chemical shifts of the complexes were referenced to the DMSO residual proton resonance as $\delta = 2.5$ ppm for DMSO-d_6. Before measurements, the ^{1}H NMR sample was heated for 2 h at 100 °C, to make the IC in a fully dissociated state in the DMSO-d_6.

2. Crystallization and Melting Behavior. DSC was employed to detect the thermal transitions and to monitor the rate of heat flow during nonisothermal/isothermal crystallization of the sample from the molten state. The weight of sample used in the DSC measurements was kept in the range of 6−8 mg. In the nonisothermal temperature program, the sample was melted at molten state (90 °C for PCL and PEG, 140 °C for PBS) for 5 min, cooled to 0 °C at a rate of 10 °C·min^{-1} and kept at 0 °C for 3min, and then heated at a rate of 10 °C min^{-1} to molten state. The crystallization temperature (T_c) and corresponding crystallization enthalpy (ΔH_c) values were taken as the peak and the area of the crystallization exotherm in the cooling run, respectively. The melting temperature (T_m) and melting enthalpy (ΔH_m) values were taken as the position of the peak and the area of the melting endotherm in the heating run, respectively. In the isothermal temperature program, after melted at molten state for 5 min, the sample was quenched to the desired crystallization temperature and the isothermal crystallization curves were recorded. The crystallization kinetics of PCL and PBS were analyzed based on these curves.

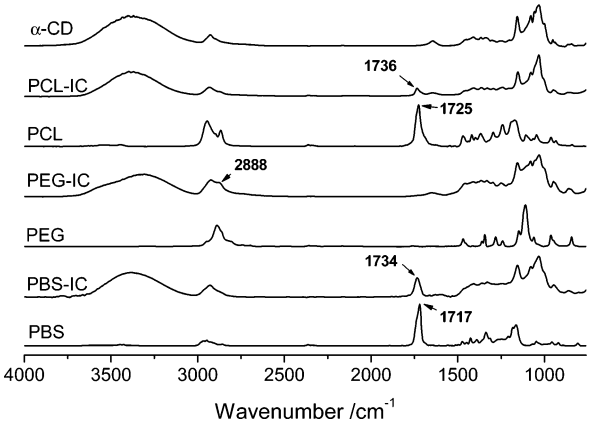

Figure 1. FT-IR spectra of α-CD, PCL, PEG, PBS, and their ICs.

Polarized optical microscopic observation was performed on an Olympus BX90 polarizing optical microscopy (POM) equipped with a digital camera. The polymer sample was placed between a microscope glass slide and a cover slip and heated on a Mettler FP82HT hot stage. The samples (about 0.2 mg) were first heated to the molten state and kept for 5 min and then quenched to the desired crystallization temperature of polymers.

Results

Formation of α-CD-ICs. α-CD-ICs were characterized by FT-IR, DSC, WAXD, and ^{1}H NMR. FT-IR observations can demonstrate the presence of both components, i.e., α-CD and polymer in each IC sample. As shown in Figure 1, the carbonyl stretching bands of PBS and PCL respectively appear at about 1717 and 1725 cm^{-1} in the their pure state. Upon complexation with α-CD, the peak tops of the carbonyl bands of PBS and PCL appear respectively at about 1734 and 1736 cm^{-1}, which shifted from the lower wavenumber crystalline region toward the higher wavenumber amorphous region,[16,17] suggesting that the crystallization of the polymer was suppressed in the α-CD-IC. The peak at 2888 cm^{-1} is assigned to the CH stretching for the PEG, and this peak also appeared in the FT-IR spectrum of PEG-IC, suggesting the presence of PEG in the PEG-IC.

Figure 2 shows the DSC thermograms of α-CD, PCL, PEG, PBS, and their ICs, and the results of DSC measurements are summarized in Table 2. α-CD does not show any detectable thermal transitions in the cooling and heating scans. As shown in Figure 2a, the melting peaks of pure PCL, PEG, and PBS were observed at 54.9, 64.9, and 113.6 °C, respectively, in the heating scan. The detectable endothermic peak could not be observed in the heating scan of PEG-IC, indicating that the crystallization of PEG was suppressed in the α-CD cavities. However, in the case of PCL-IC or PBS-IC, a very small melting peak was apparent at a slightly lower temperature than that of the pure polymers. This indicates that there is still a PCL or PBS crystalline phase outside the α-CD cavity even after IC formation and the stability of the crystal may be lower than that of the polymer crystal.

The crystallization behavior of the respective IC was measured by DSC. As shown in Figure 2b, the crystallization peaks of pure PCL, PEG, and PBS were detected at 28.2, 38.9, and 75.5 °C, respectively. Upon IC formation, the crystallization peak of PEG disappeared in the cooling scan DSC curves, also indicating that the

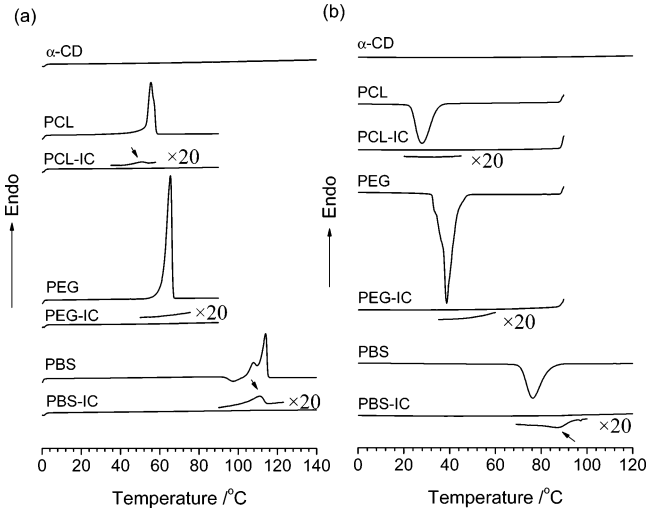

Figure 2. DSC heating (a) and cooling (b) scans of α-CD, PCL, PEG, PBS, and their ICs. The inserted curves are the corresponding enlarged DSC curves (×20).

Table 2. Crystallization and Melting Behavior of α-CD-ICs

sample	T_c/°C	ΔH_c/J/g	T_m/°C	ΔH_m/J/g
α-CD				
PCL	28.2	−75.0	54.9	76.3
PCL-IC	N.D.	N.D.	50.6	0.1
PEG	38.9	−159.4	64.9	164.8
PEG-IC	N.D.	N.D.	N.D.	N.D.
PBS	75.5	−74.4	106.8, 113.6	74.5
PBS-IC	86.4	−0.6	111.4	1.7

crystallization of the guest PEG was suppressed in the PEG-IC. In the PCL-IC, the presence of PCL crystallization could not be detect by the DSC cooling scan. However, a small crystallization peak of PBS was apparent at a higher temperature than the crystallization temperature of pure PBS, indicating the presence of the PBS chains, which can crystallize outside the CD cavity. This result may be attributed to the fact that the mobility of the uncovered part of the polymer segments should be limited by its interior part residing in the α-CD cavity, leading to the promotion of polymer crystallization.

As shown in Figure 3, the WAXD patterns of α-CD-ICs, which are quite different from those of pure polymer and α-CD components, strongly support the IC formation between α-CD and polymers. The crystalline PCL shows three prominent diffraction peaks at 21.4, 22.0, and 23.7°, PEG shows four major peaks at 18.9, 23.1, 25.9, and 26.7°, and PBS shows three strong peaks at 19.5, 21.8, and 22.4°. However, for all their α-CD-ICs, only two prominent peaks can be observed at about 19.8° and 22.5°, which are well-known to be the characteristics of α-CD-based IC crystals adopting the channel structure.[3,14,15,16,18]

The host−guest stoichiometry of the ICs was estimated by ^{1}H NMR in solution. From these signals the molar ratio of α-CD molecule to the monomeric repeat unit of polymer is calculated to be 1.9, 5.7, and 2.0 for the PCL-IC, PEG-IC, and PBS-IC, respectively. These results indicate that the polymer chains were partially covered by α-CDs in the α-CD-ICs.

Nonisothermal Crystallization Behavior. The nucleating effects of talc, α-CD, and α-CD-ICs on the crystallization of semicrystalline polymers (PCL, PEG, and PBS) were investigated by DSC nonisothermal

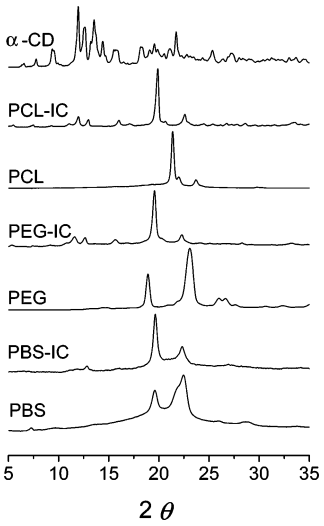

Figure 3. WAXD patterns of α-CD, PCL, PEG, PBS, and their ICs.

crystallization process. All samples were melted at molten state of polymers (90 °C for PCL and PEG, 140 °C for PBS) for 5 min to erase the thermal history residing in the samples. In Figure 4, the DSC cooling scan of these melted samples at 10 °C min^{-1} reveals the relative nucleation abilities of talc, α-CD, and α-CD-ICs, as indicated by the peak crystallization temperature (T_c) and the temperature range over which they crystallized. Usually, a high T_c and a narrow crystallization temperature range indicate faster crystallization. In Table 3 are summarized the values of T_cs and the corresponding crystallization enthalpies of polymers measured during cooling scans.

As shown in Figure 4a, the T_c value of PCL, which is about 28.2 °C in the pure state, shifts to a higher temperature with the addition of talc, α-CD, and α-CD-ICs, indicating their nucleation effects on the crystallization of PCL. The T_c value for pure PCL and those for PCL in the PCL blends with talc, α-CD, and α-CD-ICs increase in the order of PCL < PCL/PEG-IC 2 wt % ≈ PCL/α-CD 2 wt % < PCL/PBS-IC 2 wt % < PCL/PCL-IC 2 wt % < PCL/talc 2 wt %. Among the ICs, the most effective nucleating agent is PCL-IC, which shifts the T_c of PCL to 36.5 °C. This is almost 8 °C higher than that of pure PCL, confirming that the nucleation effect of the PCL-IC on the crystallization behavior of PCL was significantly larger than those of pure α-CD and the other kinds of α-CD-ICs.

As shown in Figure 4b, the T_c value of pure PEG is about 38.9 °C, and the crystallization proceeds within a broad temperature range. Although the crystallization rate of the PEG is very fast and the crystallization temperature is very high, with an addition of the nucleation agents, the T_c of PEG increases and the crystallization process finishes within a narrow temperature range. It is worth noting that the crystallization rate of PEG with PEG-IC is faster than that of PEG with other nucleating agents.

As shown in Figure 4c, the T_c value of pure PBS is about 75.5 °C and the crystallization proceeds in a broad temperature range. The T_c value for PBS and those for PBS in the PBS blends with talc, α-CD, and α-CD-ICs increase in the order of PBS ≈ PBS/PCL-IC 2 wt % < PBS/PEG-IC 2 wt % < PBS/α-CD 2 wt % < PBS/talc 2 wt %< PBS/PBS-IC 2 wt %. The 2 wt % talc can enhance the crystallization of PBS, but such an effect was less

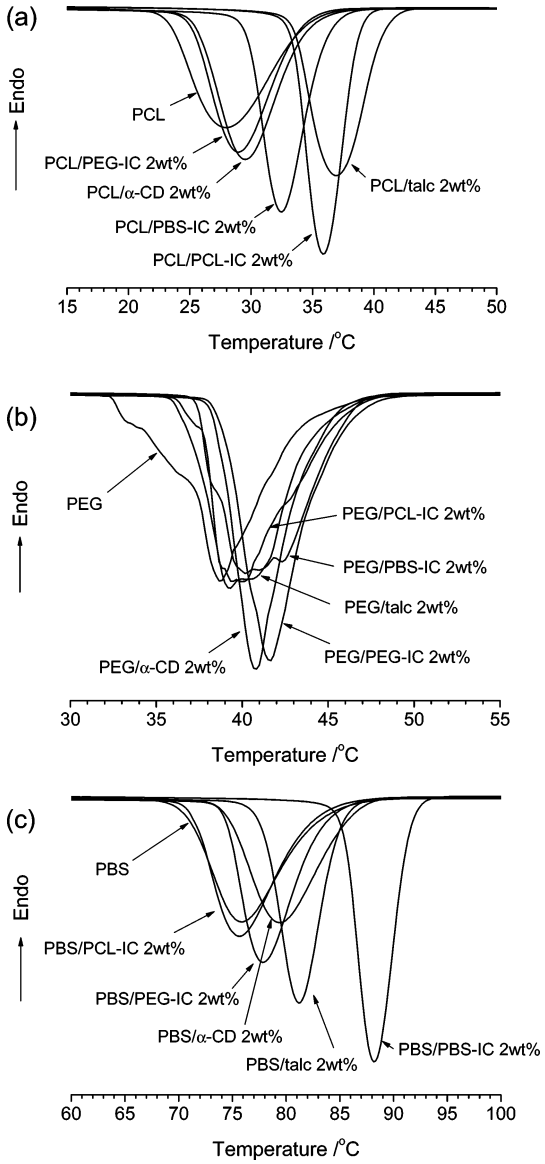

Figure 4. DSC nonisothermal crystallization curves of PCL (a), PEG (b) and PBS (c) containing 2 wt % talc, α-CD, PCL-IC, PEG-IC, and PBS-IC. The cooling rate is 10 °C/min. Before the cooling, the samples were melted at molten state of polymers (90 °C for PCL and PEG, 140 °C for PBS) for 5 min to erase the thermal history.

than that caused by PBS-IC, which is the most effective nucleation agent, shifting the T_c of PBS to 88.4 °C. This is almost 13 °C higher than that of pure PBS. Moreover, it is noted that PBS in the PBS/PBS-IC 2 wt % blend crystallizes in the much narrow temperature range, and the crystallization enthalpy ΔH_c of PBS is the most greatly increased by the addition of PBS-IC (Table 3), confirming that the nucleation effect of the PBS-IC on the crystallization behavior of PBS was significantly larger than those of pure α-CD and the other kinds of α-CD-ICs. These results suggest that the IC of a given polymer could greatly enhance the nucleation and crystallization of the polymer itself.

Isothermal Crystallization Behavior. In Figure 5 are presented the DSC thermograms of isothermal crystallization of PCL and PBS containing nucleating agents at 44 and 90 °C, respectively. Clearly, the isothermal crystallization rate of polymer containing its α-CD-IC is much higher than that of the pure polymer, confirming again the IC of a given polymer enhances

Table 3. Nonisotheramal Crystallization and Melting Behavior of PCL, PEG, and PBS Containing 2 wt % Nucleating Agents

sample	T_c/ °C	ΔH_c/ J/g	T_m1/ °C	T_m2/ °C	T_m3/ °C	ΔH_m/ J/g	X_c/ %
PCL	28.2	−75.0		54.9		76.3	46.0
PCL/talc 2wt%	37.1	−74.8		54.7		75.1	45.2
PCL/α-CD 2wt%	29.7	−75.5		54.1		76.1	45.9
PCL/PCL-IC 2wt%	36.5	−76.6		54.9		77.2	46.5
PCL/PEG-IC 2wt%	29.3	−74.0		54.7		74.1	44.6
PCL/PBS-IC 2wt%	32.6	−74.8		54.2		74.8	45.1
PEG	38.9	−159.4	64.9			164.8	79.2
PEG/talc 2wt%	40.1	−158.5	64.6			166.3	80.0
PEG/α-CD 2wt%	42.1	−158.7	64.0			166.8	80.2
PEG/PCL-IC 2wt%	40.0	−155.9	64.5			166.3	80.0
PEG/PEG-IC 2wt%	40.4	−156.8	63.7			167.2	80.4
PEG/PBS-IC 2wt%	41.1	−156.4	64.6			164.8	79.2
PBS	75.5	−74.4	113.6	106.8		74.5	37.3
PBS/talc 2wt%	81.4	−74.5	113.9	107.6		74.9	37.4
PBS/α-CD 2wt%	79.7	−75.0	113.4	107.9		75.2	37.6
PBS/PCL-IC 2wt%	75.8	−74.0	113.6	107.0		74.3	37.1
PBS/PEG-IC 2wt%	77.7	−74.7	114.1	105.8		75.3	37.7
PBS/PBS-IC 2wt%	88.4	−82.3	113.2	109.7	102.3	84.2	42.1

effectively the crystallization of the polymer itself. The results for isothermal crystallization of PEG were not shown here. The distinct feature for the PEG is the multiple crystallization peak during the isothermal crystallization process; thus, the Avrami treatment cannot be applied to this complicated crystallization processes. This may be due to the presence of a low-molecular weight PEG fraction. A transient nonintegral folding crystal and an integral folding crystal should have been formed in this isothermal crystallization stage.[19]

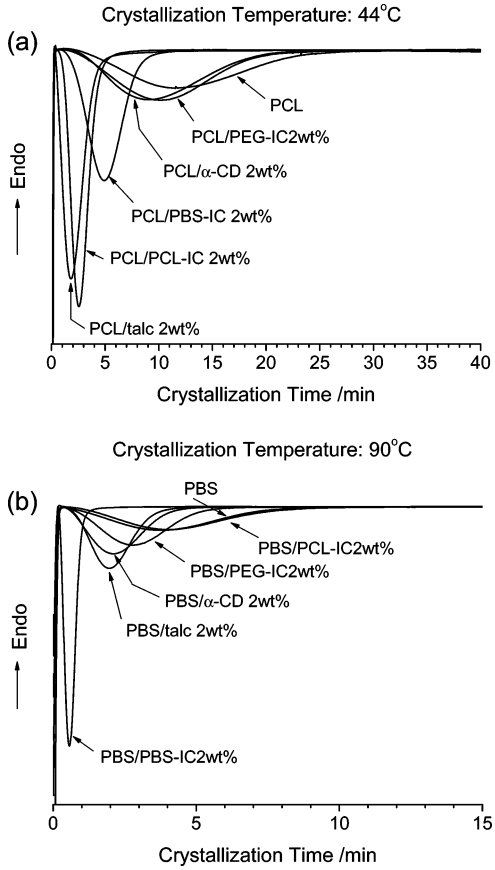

Figure 5. DSC isothermal crystallization curves of PCL and PBS containing 2 wt % nucleating agents (talc, α-CD, PCL-IC, PEG-IC, and PBS-IC). The samples were melted at molten state of polymers (90 °C for PCL and PEG, 140 °C for PBS) for 5 min to erase the thermal history.

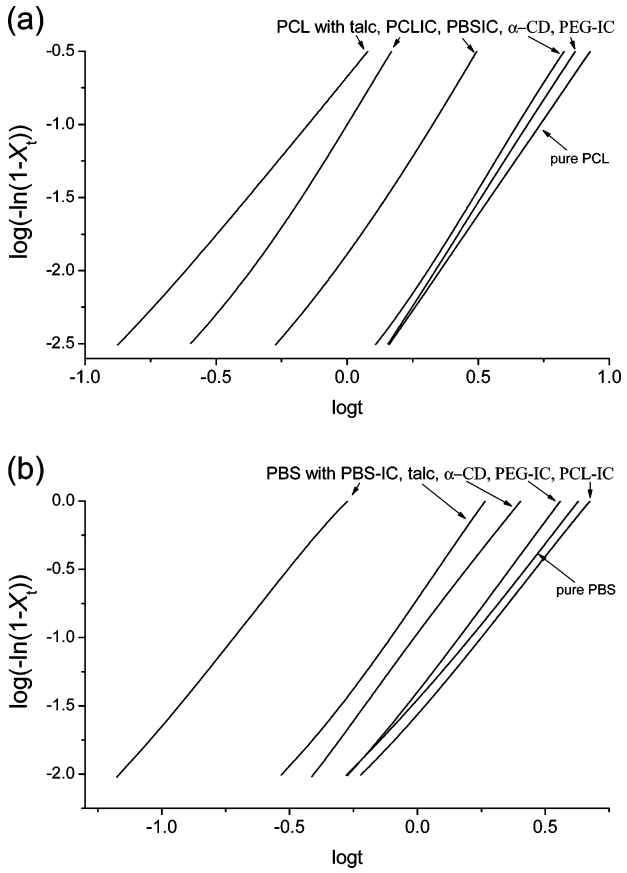

Figure 6. Avrami plots of the isothermal crystallization of PCL and PBS containing 2 wt % nucleating agents (talc, α-CD, PCL-IC, PEG-IC, and PBS-IC) at 44 and 90 °C, respectively.

Crystallization kinetics was determined from the isothermal DSC measurements. The isothermal heat flow curve was integrated to determine the degree of crystallinity of the sample as a function of crystallization time. The relative crystallinity X_t at any given time was calculated from the integrated area of the DSC curve from $t = 0$ to $t = t$ divided by the integrated area of the whole heat flow curve. The isothermal bulk crystallization kinetics was analyzed with the Avrami equation[20]

$$X_t = 1 - \exp(-kt^n) \tag{1}$$

where n is an index related to the dimensional growth and the way of formation of primary nuclei and k is the overall rate constant associated with both nucleation and growth contributions. The linear form of eq 1 is given as eq 2

$$\log[-\ln(1 - X_t)] = \log k + n \log t \tag{2}$$

n and k are obtained by plotting $\log[-\ln(1 - X_t)]$ against $\log t$. As an example, Figure 6 illustrates the plots of $\log[-\ln(1 - X_t)]$ vs $\log t$ and the linear fitting of data for the PCL and PBS samples crystallized at 44 and 90 °C, respectively. Meanwhile, the crystallization half-time $t_{1/2}$, which is defined as the time when the crystallinity arrives at 50%, can be determined from the kinetics parameters measured by using the following equation:

$$t_{1/2} = \left(\frac{\ln 2}{k}\right)^{1/n} \tag{3}$$

Table 4. Kinetic Parameters of Isothermal Crystallization of PCL and PBS[a]

	42			44			46		
iso. cry. temp./°C parameter	n	$k \times 10^3$	$t_{1/2}$	n	$k \times 10^3$	$t_{1/2}$	n	$k \times 10^3$	$t_{1/2}$
PCL	2.80	4.68	5.98	2.54	1.33	11.79	2.39	0.39	22.95
PCL/talc 2wt%	2.01	894.75	0.88	2.08	210.04	1.78	2.26	32.40	3.88
PCL/α-CD 2wt%	2.65	11.40	4.71	2.63	1.85	9.53	2.86	0.12	20.86
PCL/PCL-IC 2wt%	2.52	652.68	1.02	2.75	104.09	1.99	2.94	9.09	4.37
PCL/PEG-IC 2wt%	2.69	9.78	4.86	2.72	1.29	10.08	2.66	0.21	21.34
PCL/PBS-IC 2wt%	2.38	123.48	1.90	2.63	16.57	4.13	2.95	0.49	11.64
	90			92			94		
iso. cry. temp./°C parameter	n	$k \times 10^3$	$t_{1/2}$	n	$k \times 10^3$	$t_{1/2}$	n	$k \times 10^3$	$t_{1/2}$
PBS	2.32	32.20	3.75	2.36	10.60	5.88	2.56	2.85	8.55
PBS/talc 2wt%	2.60	194.89	1.63	2.89	27.77	3.04	2.97	4.33	5.51
PBS/α-CD 2wt%	2.34	102.60	2.26	2.45	32.80	3.47	2.62	8.22	5.43
PBS/PCL-IC 2wt%	1.97	66.10	3.29	2.17	21.41	4.96	2.23	6.79	7.98
PBS/PEG-IC 2wt%	2.55	61.07	2.59	2.79	12.73	4.20	2.84	2.88	6.89
PBS/PBS-IC 2wt%	2.27	4339.10	0.45	2.55	2446.81	0.61	2.96	740.63	0.98

[a] The units for k and $t_{1/2}$ are min^{-n} and min, respectively.

As shown in Figure 6a,b, the nearly parallel curves were observed for the PCL and PBS samples, respectively. The crystallization parameters k, n, and $t_{1/2}$ are listed in Table 4. For all of the PCL samples, the Avrami exponent value n ranges from 2 to 3, whereas it is almost insensitive to the addition of nucleation agents. The kinetic constants k and $t_{1/2}$ show strong dependence on the crystallization temperature. With increasing the crystallization temperature, the value of k decreases, whereas that of $t_{1/2}$ increases. These results indicate that, with increasing crystallization temperature, the crystallization rate decreases. The value of k increases in the order of PCL < PCL/PEG-IC 2 wt % < PCL/α-CD 2 wt % < PCL/PBS-IC 2 wt % < PCL/PCL-IC 2 wt % < PCL/talc 2 wt %, whereas that of $t_{1/2}$ decreases in the reverse trend. Clearly, talc and PCL-IC were the good effective nucleating agents on the crystallization of PCL.

For all of the PBS samples, the Avrami exponent value n is similar at a given temperature. Also, the value of k increases with decreasing crystallization temperature, whereas the $t_{1/2}$ value increases with increasing temperature. The value of $t_{1/2}$ decreases in the order of PBS ≈ PBS/PCL-IC 2 wt % > PBS/PEG-IC 2 wt % > PBS/α-CD 2 wt % > PBS/talc 2 wt % > PBS/PBS-IC 2 wt %. Clearly, PBS-IC was the most effective nucleating agent on the crystallization of PBS.

Melting Behavior. Figure 7 shows the DSC heat flow curves of PCL, PEG, and PBS samples after nonisothermal crystallization processes, and their thermal data are summarized in Table 3. The crystallinity of the polymer was calculated from $\Delta H_m/\Delta H°$, where $\Delta H°$ is the melting enthalpy expected for a polymer with 100% crystallinity, here, assuming the heats of fusion $\Delta H°$ of PCL, PEG, and PBS are 166,[21] 208,[22] and 200 J/g,[23] respectively.

As shown in Figure 7a, the double melting temperatures, T_m1 and T_m2, were detected for the PCL samples on the DSC heating traces. The nucleating agents forced the peak of T_m1 to increase and depressed the T_m2 peak. The ratio of the peak area between the melting peaks of T_m1 and T_m2 for the PCL containing nucleating agents and pure PCL are different; the increment of the ratio of peak area between the peaks of T_m2 and T_m1 was enhanced as the nucleation effect of the nucleating agent was improved. As seen in Table 3, although, the crystallization enthalpy and the heat of fusion are not very sensitive to the addition of the PCL-IC, it also seems that high crystallization enthalpy and heat of

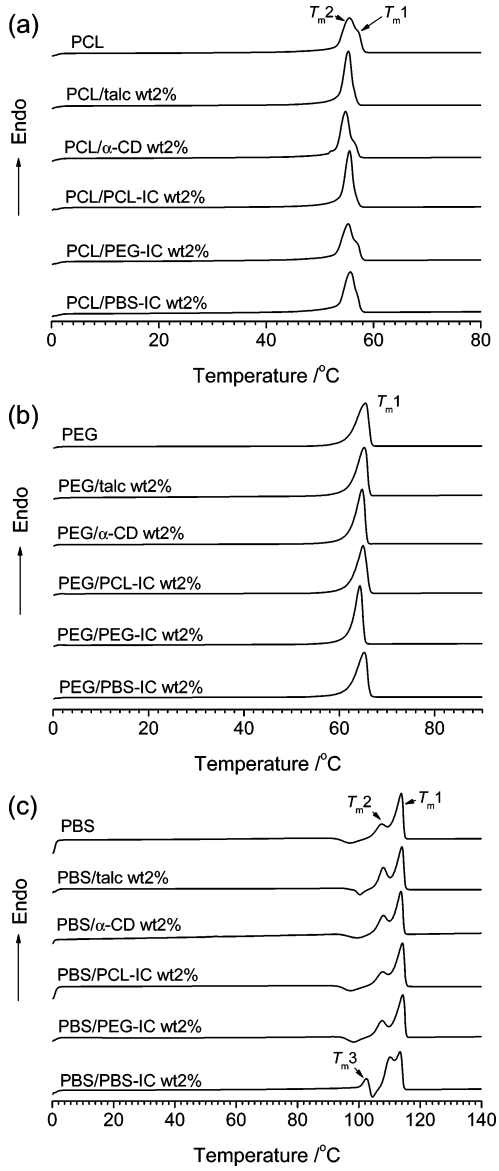

Figure 7. Melting behavior of PCL, PEG and PBS containing 2 wt % nucleating agents (talc, α-CD, PCL-IC, PEG-IC, and PBS-IC) at a heating rate of 10 °C/min after nonisothermal crystallization process.

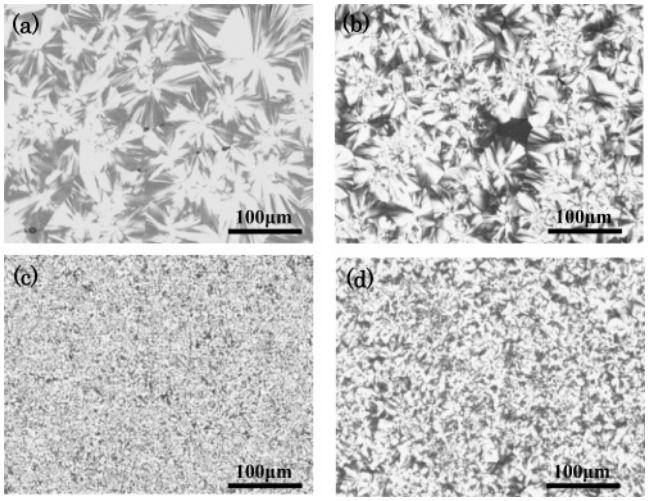

Figure 8. Polarized optical micrographs of PCL (a), and PCL containing 2 wt % α-CD (b), talc (c), PCL-IC (d).

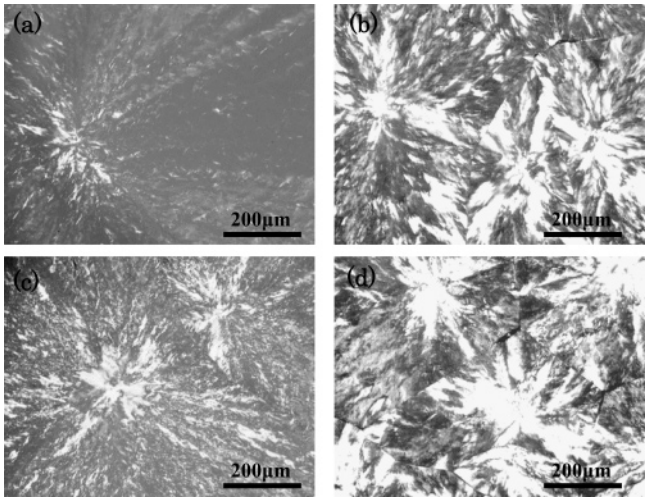

Figure 9. Polarized optical micrographs of PEG (a), and PEG containing 2 wt % α-CD (b), talc (c), PEG-IC (d).

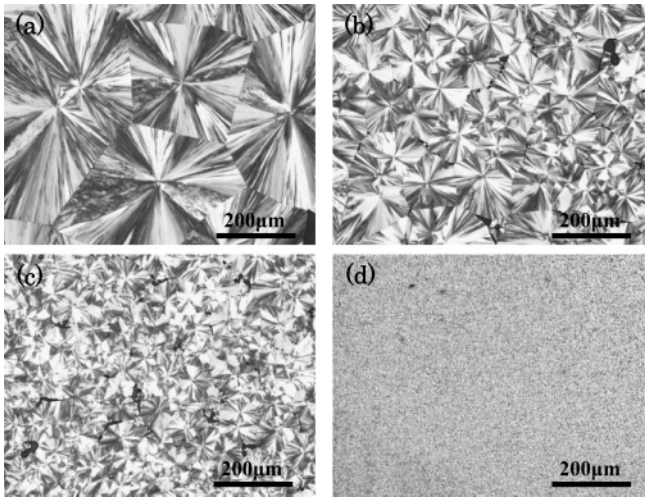

Figure 10. Polarized optical micrographs of PBS (a), and PBS containing 2 wt % α-CD (b), talc (c), PBS-IC (d).

fusion values are related with a high crystallization temperature.

As shown in Figure 7b, only one melting point was detected for PEG and PEG with nucleating agents, and the crystallization enthalpy and the heat of fusion were not very sensitive to the addition of the nucleation agents. However, it should be noted that the melting peak of PEG with addition of nucleating agents is slightly shaper than that of the PEG. These results may be due to the increased crystallization rate and the improved perfectness of the PEG crystals with addition of the nucleating agents.

The distinct feature for the melting behavior of PBS is that the PBS crystals partially melted and recrystallized during heating process as shown in Figure 7c. Here, T_m1, T_m2, and T_m3 indicate the melting peaks. The peak temperature of T_m1 observed at the highest temperature (ca. 114 °C) is independent of the addition of nucleating agents, because it corresponds to the melting of crystals recrystallized during the heating process.[24] The T_m2 and T_m3 peaks are possibly attributed to the melting of original crystallites corresponding to the two kinds of morphologically different crystalline phases despite the same crystalline structure, i.e., α-form of PBS.[24] As shown in Figure 7c and Table 3, the heat flow curve of pure PBS exhibits the lowest T_m3 and T_m2 values, indicating the formation of a crystalline phase with the worst crystal perfectness or the thinnest lamella thickness. On the other hand, it is noted that the more effective nucleation agent was used, the higher T_m2 and T_m3 values can be observed. With the addition of PBS-IC, PBS shows the most intense T_m2 and T_m3 peaks. The crystallinity of PBS is not very sensitive to the addition of the nucleation agents, as shown in Table 3. However, it also seems that high crystallinity is related to a high T_c value measured during cooling.

Spherulitic Morphology. In Figure 8 are shown the spherulitic morphologies of pure PCL and PCL containing nucleating agents crystallized at 42 °C after quenched directly from 90 °C. The diameter of pure PCL spherulites reaches up to 100 μm before they impinge with each other. With the addition of nucleation agents, the number of nuclei will increase and the average diameter of spherulites will reduce. The diameter of spherulite decreased in the order of PCL > PCL/α-CD 2 wt % > PCL/PCL-IC 2 wt % > PCL/talc 2 wt %, whereas the nucleation density increased in the reverse trend, in good accordance with the DSC results. Obviously, the PCL-IC acts as a good nucleating agent for the PCL crystallization. Similar results were observed in the PEG and PBS blends with nucleating agents. Also as shown in Figures 9 and 10, the PEG-IC and PBS-IC greatly increases the nucleation density for PEG and PBS crystallization, respectively.

Discussion

The crystallization behavior of polymers in the blend is affected by many factors, such as composition, thermal history, interfacial interactions, size, and its distribution of dispersed particles. The crystallization process of polymers from the molten state can be divided into two stages, that is, the nucleation and the crystal growth. A primary nucleation process may be either homogeneous or heterogeneous.[25] The homogeneous nucleation occurs sporadically in the melt by thermal fluctuation, whereas the latter starts on the surface of microscopic insoluble particles dispersed randomly in the polymer melt, such as impurities or nucleating agents arbitrarily added. In practice, however, unless under very special conditions, it is rare to observe homogeneous nucleation for crystalline polymers. Whenever there is nucleating agent present in a polymer melt,

it can affect the free energy balance for nucleation, usually so as to increase the nucleation rate and prevent homogeneous nucleation. For heterogeneous nucleation, due to a much reduced surface energy, the nucleation rate can increase by several orders of magnitude. Therefore, the effect of homogeneous nucleation can be totally smeared by heterogeneous nucleation and becomes inaccessible experimentally. So far in the above discussion, it has been assumed that the heterogeneous nucleation is achieved via foreign surfaces, and the presence of these high energy surfaces can favorably affect the free energy balance for nucleation of crystalline polymers.

In the case of the present study, α-CD-ICs, used as the nucleating agent for crystalline polymers, PCL, PEG, and PBS, show different nucleation abilities on the different polymers. From the structural analysis of PCL-IC, PEG-IC, and PBS-IC, the long polymer chains were found to be partially included inside the α-CD cavities. Therefore, the polymer chains in the bulk phase may contact not only the exterior of α-CD macrocycle but also the end parts of polymer chains protruding from the α-CD cavity and/or the free chain segments uncovered by α-CD. A possible explanation can be given to this interesting phenomenon, that is, the difference in the interfacial interaction between bulk polymers and nucleating agents should be responsible for the difference in the nucleation effects.

As described above, a very interesting phenomenon was that the IC of the polymer can greatly enhance the nucleation and crystallization of the polymer itself, as the kind of polymers in the ICs are the same as those surrounding the ICs. This result is also supported by our previous work,[9] with the PHB forms its IC, a large increase of T_c (about 33 °C) can be observed during the cooling process from the melt. This may be attributable to the fact that the mobility of the uncovered part of the polymer segments should be limited by its interior part residing in the α-CD cavity, leading to the nucleation of the polymer. A slightly closer packing of polymer chains in the vicinity of a foreign surface makes the transport of polymer chain segments during crystallization easy. Therefore, this high-energy interior surface of α-CD can favorably affect the free energy balance for nucleation.

However, PBS-IC can greatly enhance the crystallization of bulk PBS, whereas PCL-IC and PEG-IC have fewer nucleation effects on the crystallization of bulk PBS. This may be caused by miscibility between PBS and nucleating agents. The crystallization temperature of PBS is above 75 °C, which is above the melting temperatures of PCL and PEG. Thus during the nonisothermal crystallization, when the PBS crystallization has finished, uncovered PCL and PEG chains still remain in the amorphous state. As PCL and PBS are immiscible in the amorphous state,[26] the PBS chains cannot contact intimately the uncovered PCL segments of the PCL-IC. Thus, the PCL-IC particles have a tendency to separate from the molten PBS, and cannot induce the nucleation of the PBS crystallization. In contrast, PBS and PEG are miscible in the molten state;[25,27] thus, it seems that the PBS chains are able to close enough to the particle of PEG-IC to be induced nucleation. This approach of PBS chains onto the surface of the PEG-IC particle, due to polar interaction, causes a reduction of the surface energy barrier and increases the nucleation density for PBS crystallization. Namely, the miscibility between the polymers protruding from the α-CD cavity of ICs and those surrounding ICs seem to be related to the nucleation effects of ICs. The higher the miscibility, the more effective the nucleation agent.

Although, the PCL-IC particle cannot act as the nucleating agent on the crystallization of PBS, the PBS-IC has a good nucleating effect on the crystallization of PCL. This nucleation mechanism might be different from that of the PCL-IC particle in the bulk phase PBS. As shown in Figure 2a, the crystallization of PCL will be start below 45 °C, a portion of uncovered PBS chains in the ICs already crystallized at about 86 °C. Meanwhile, the PCL may be epitaxially crystallized[28] on the surface of crystallized PBS, which is acting as the true nucleating agent to initiate nucleation.

Moreover, the complexed state of α-CD is more effective for promoting the crystallization of the polymer itself, but free sate α-CD also enhances the nucleation and crystallization of polymers. The above discussion also can give a reasonable explanation for the nucleation effect of pure α-CD, and it may be attributable to two possible reasons. The most plausible one in the present case is that some polymer chains may partially and spontaneously penetrate into the cavity of α-CD during blending with α-CDs or melting α-CD/polymer samples, leading to the formation of inclusion complexes with α-CDs. Similar to the end of the polymer protruding from the α-CD cavity and the free chain segments uncovered by α-CD in ICs, the free segment adjacent to that covered by α-CD in the poorly included chains may induce the nucleation of the polymer. This assumption is indirectly supported by the researches of Peet and Harada et al.;[29] that is, the solid-state α-CD added to the liquid state of PEG can form crystalline α-CD-PEG-IC. However, as the ability to form the inclusion complex in the molten state or during the blending is small, the nucleation effect of α-CD cannot be as effective as α-CD ICs. The other reason is that the different crystalline structure of α-CD might be lead to different nucleation abilities. X-ray analysis (Figure 3) shows that the complexed state of α-CD adopts the channel structure, whereas that of the free state adopts the cage structure. A variety of results (for examples: PCL-IC has no nucleation effect on the crystallization of PBS; α-CD including different polymers appears to have different nucleation abilities) prove that the channel structure of the α-CD-complex particles affects less the crystallization of PCL, PEG, and PBS. However, we should not eliminate the possibility of epitaxial crystallization of polymers on the surface of α-CD particles.

Conclusion

Polymeric inclusion complexes between α-CD and semicrystalline polymers (PCL, PEG, and PBS) were successfully prepared and characterized quantitatively with various analytical methods. The WAXD studies showed that all of the α-CD-ICs adopt a channel structure. Both DSC and ^{1}H NMR results suggested that the polymer chains were partially complexed by α-CDs. Thus, the polymer chains in the bulk phase can contact not only the exterior of the α-CD macrocycle but also the end parts of polymer chains protruding from the α-CD cavity and/or the free chain segments uncovered by α-CD, when the α-CD-IC as a nucleating agent is added into the semicrystalline polymers. Therefore, the difference in the interfacial interaction between bulk

polymers and the nucleating agents should be responsible for the difference in the nucleation effects. The nucleation effect of α-CD on the crystallization of PCL, PEG, and PBS was also investigated with DSC and POM. We found that the α-CD-IC of a given polymer could effectively enhance the crystallization of the polymer itself, demonstrating that the α-CD in the complex state is more effective for promoting the crystallization of the polymer than for promoting the free state α-CD. This result may be attributable to the limited mobility of the uncovered part of the polymer segments constrained by its interior part residing in the α-CD cavity, leading to the nucleation of polymer crystallization.

References and Notes

(1) (a) Doi, Y. *Microbial Polyesters*; VCH: New York, 1990. (b) Inoue, Y.; Yoshie, N. *Prog. Polym. Sci*. **1992**, *17*, 571.

(2) Richard, A. G.; Bhanu, K. *Science* **2002**, *297*, 803.

(3) (a) Harada, A.; Kamach, M. *Macromolecules* **1990**, *23*, 2821. (b) Harada, A.; Li, J.; Kamachi, M. *Nature* **1992**, *356*, 325.

(4) (a) Rusa, C. C.; Tonelli, A. E. *Macromolecules* **2000**, *33*, 5321. (b) Shuai, X.; Porbeni, F. E.; Wei, M.; Shin, I. D.; Tonelli, A. E. *Macromolecules* **2001**, *34*, 7355. (c) Rusa, C. C.; Wei, M.; Shuai, X.; Bullions, T. A.; Wang, X.; Rusa, M.; Uyar, T.; Tonelli, A. E. *J. Polym. Sci., Part B: Polym. Phys.* **2004**, *42*, 4207. (d) Shuai, X.; Porbeni, F. E.; Wei, M.; Bullions, T.; Tonelli, A. E. *Macromolecules* **2002**, *35*, 3126. (e) Jia, X.; Wang, X.; Tonelli, A. E.; White, J. L. *Macromolecules* **2005**, *38*, 2775.

(5) Shuai, X.; Wei, M.; Porbeni, F. E.; Bullions, T. A.; Tonelli, A. E. *Biomacromolecules* **2002**, *3*, 201.

(6) (a) Wei, M.; Shuai, X.; Tonelli, A. E. *Biomacromolecules* **2003**, *4*, 783. (b) Shuai, X.; Porbeni, F. E.; Wei, M.; Bullions, T.; Tonelli, A. E. *Macromolecules* **2002**, *35*, 2401. (c) Wei, M.; Davis, W.; Urban, B.; Song, Y.; Porbeni, F. E.; Wang, X.; White, J. L.; Balik, C. M.; Rusa, C. C.; Fox, J.; Tonelli, A. E. *Macromolecules* **2002**, *35*, 8039. (d) Rusa, C. C.; Wei, M.; Bullions, T. A.; Rusa, M.; Gomez, M. A.; Porbeni, F. E.; Wang, X.; Shin, I. D.; Balik, C. M.; White, J. L.; Tonelli, A. E. *Cryst. Growth Des.* **2004**, *4*, 1431.

(7) (a) Anderson, A. J.; Dawes, E. A. *Microbiol. Rev.* **1990**, *54*, 450. (b) Steinbüchel, A. *Biopolymers*; Wiley-VCH: Weinheim, Germany, 2001; Vols. 3 and 4. (c) Avella, M.; Immirzi, B.; Malinconico, M.; Martuscelli, E.; Volpe, M. G. *Polym. Int.* **1996**, *39*, 191. (d) Holmes, P. A. In *Development of Crystalline Polymers*; Bassett, D. C., Ed.; Elsevier: London, 1988; Vol. 2, p 1.

(8) (a) El-Hadi, A.; Schnabel, R.; Straube, E.; Müller, G.; Henning, S. *Polym. Test.* **2002**, *21*, 665. (b) Barham, P. J.; Keller, A. *J. Polym. Sci., Polym. Phys. Ed.* **1986**, *24*, 69.

(9) (a) He, Y.; Inoue, Y. *Biomacromolecules* **2003**, *4*, 1865. (b) He, Y.; Inoue, Y. *J. Polym. Sci., Part B: Polym. Phys.* **2004**, *42*, 3461.

(10) Liu, W. J.; Yang, H. L.; Wang, Z.; Dong, L. S.; Liu, J. J. *J. Appl. Polym. Sci.* **2002**, *86*, 2145.

(11) Hollinger, M. A. *Toxicol. Lett.* **1990**, *52*, 121.

(12) (a) Wenz, G. *Angew. Chem., Int. Ed. Engl*. **1994**, *33*, 803. (b) Bender, M. L.; Komiyama, M. *Cyclodextrin Chemistry*; Springer-Verlag: Berlin, 1978. (c) Szejtli, J. *Cyclodextrins and Their Inclusion Complexes*; Akademiai Kiado: Budapest, 1982. (d) Inoue, Y.; *Ann. Rep. NMR Spectrosc*. **1993**, *27*, 59. (e) Harada, A. In *Large Ring Molecules*; Semlyen, J. A., Ed.; Wiley: Chichester, U.K., 1996; p 407.

(13) Ishioka, R.; Kitakuni, E.; Ichikawa, Y. In *Biopolymers: Vol. 4, Polyesters III*; Doi, Y., Steinbüchel, A., Eds.; Wiley-VCH: Chichester, U.K., 2002.

(14) Huang, L.; Allen, E.; Tonelli, A. E. *Polymer* **1998**, *39*, 4857.

(15) Shin, K.; Dong, T.; He, Y.; Inoue. Y. *Macromol. Biosci*. **2004**, *4*, 1075.

(16) Dong, T.; He, Y.; Shin, K.; Inoue, Y. *Macromol. Biosci*. **2004**, *4*, 1084.

(17) He, Y.; Inoue, Y. *Polym. Int*. **2000**, *49*, 623.

(18) (a) McMullan, R. K.; Saenger, W.; Fayos, J.; Mootz, D. *Carbhydr. Res*. **1973**, *31*, 37. (b) Takeo, K.; Kuge, T. *Agric. Biol. Chem.* **1970**, *34*, 1787.

(19) (a) Cheng, S. Z. D.; Zheng, A.; Chen, J.; Heberer, D. P. *J. Polym. Sci., Part B: Polym. Phys.* **1991**, *29*, 287. (b) Cheng, S. Z. D.; Zheng, A.; Chen, J.; Heberer, D. P. *J. Polym. Sci., Part B: Polym. Phys.* **1991**, *29*, 299.

(20) (a) Avrami, M. J. *Chem. Phys*. **1939**, *7*, 1103. (b) Avrami, M. J. *Chem. Phys*. **1940**, *8*, 212. (c) Avrami, M. J. *Chem. Phys*. **1941**, *9*, 177.

(21) El-Hadi, A.; Schinabel, R.; Staube, E.; Mueller, A.; Henning S. *Polym. Test* **2002**, *21*, 665.

(22) (a) Campbell, C.; Viras, K.; Richardson, M. J.; Masters, A. J.; Booth, C. *Makromol. Chem*. **1993**, *194*, 799. (b) Yang, Z.; Yu, G. E.; Cooke, J.; Ali-Adib, Z.; Viras, K.; Matsuura, H.; Ryan, A. J.; Booth, C. J. *Chem. Soc., Faraday Trans*. **1996**, *92*, 3173. (c) Cooke, J.; Viras, K.; Yu, G. E.; Sun, T.; Yonemitsu, T.; Ryan, A. J.; Price, C.; Booth, C. *Macromolecules* **1998**, *31*, 3030. (d) Xu, J.; Fairclough, J. P. A.; Mai, S.; Ryan, A. J.; Chaibundit, C. *Macromolecules* **2002**, *35*, 6937.

(23) Miyata, T.; Masuko, T. *Polymer* **1998**, *39*, 1399.

(24) (a) Yoo, E. S.; Im, S. S. *J. Polym. Sci., Part B: Polym. Phys.* **1999**, *37*, 1357. (b) Gan, Z.; Abe, H.; Doi, Y. *Biomacromolecules* **2001**, *2*, 313.

(25) He, Y.; Zhu, B.; Kai, W.; Inoue, Y. *Macromolecules* **2004**, *37*, 3337.

(26) Qiu, Z.; Komura, M.; Ikehara, T.; Nishi, T. *Polymer* **2003**, *44*, 7749.

(27) Qiu, Z.; Ikehara, T.; Nishi, T. *Polymer* **2003**, *44*, 2799.

(28) Mercier, J. P. *Polym. Eng. Sci.* **1990**, *30*, 270.

(29) (a) Peet, J.; Rusa, C. C.; Hunt, M. A.; Tonelli, A. E.; Balik, C. M. *Macromolecules* **2005**, *38*, 537. (b) Harada, A.; Okada, M.; Kawaguchi, Y. *Chem. Lett.* **2005**, *34*, 542.

MA050826R